

Supplement of Atmos. Meas. Tech., 13, 4159–4167, 2020
<https://doi.org/10.5194/amt-13-4159-2020-supplement>
© Author(s) 2020. This work is distributed under
the Creative Commons Attribution 4.0 License.



Supplement of

A compact, high-purity source of HONO validated by Fourier transform infrared and thermal-dissociation cavity ring-down spectroscopy

Nicholas J. Gingerysty and Hans D. Osthoff

Correspondence to: Hans D. Osthoff (hosthoff@ucalgary.ca)

The copyright of individual parts of the supplement might differ from the CC BY 4.0 License.

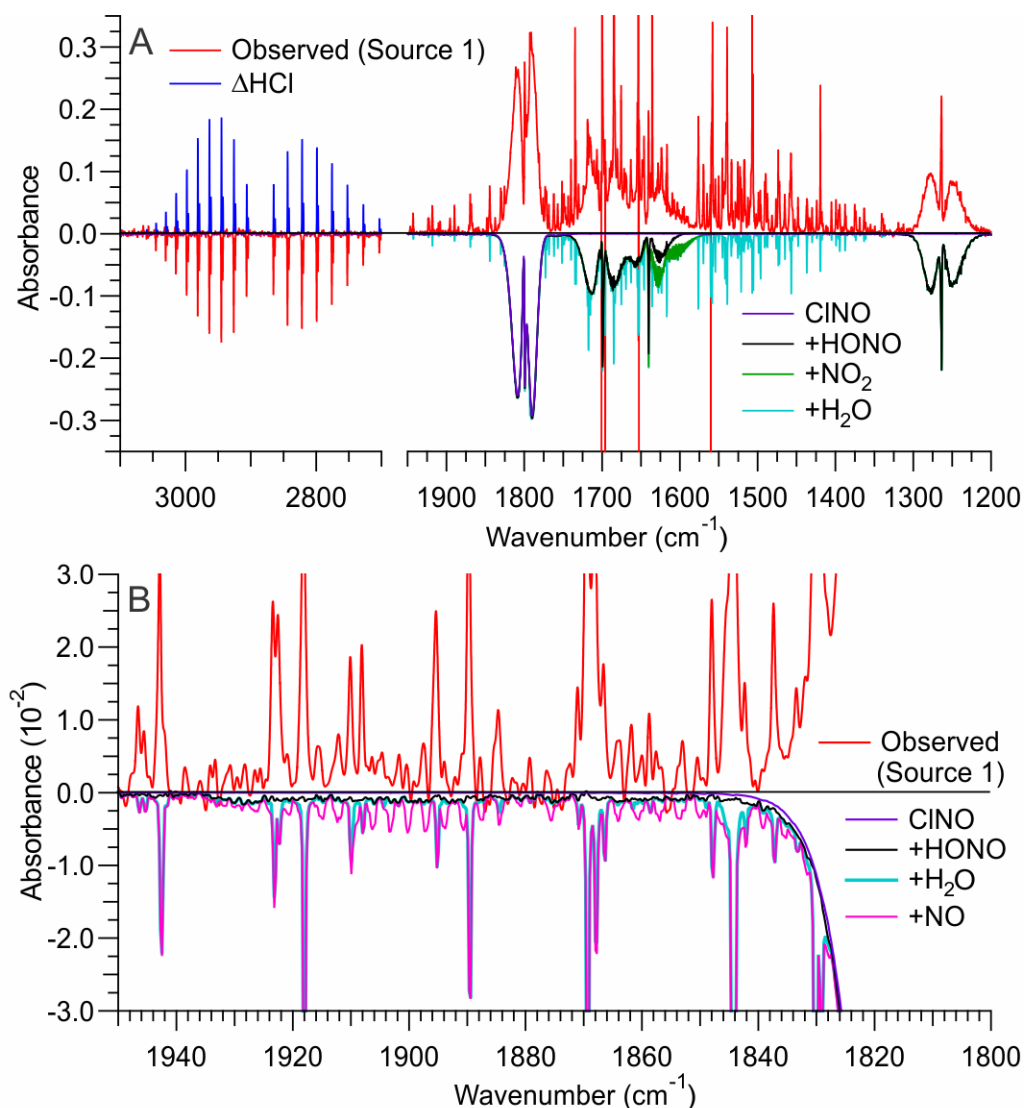


Figure S1. (A) Infrared spectrum (shown in red colour) of a gas stream generated by reaction of $\text{HCl}_{(g)}$ with $\text{NaNO}_{2(s)}$ using source 1. The reference spectrum was collected when NaNO_2 was bypassed, i.e., contained HCl . The transmission spectrum (not shown) was void of HCl lines, indicating quantitative conversion of HCl . Literature spectra (Sharpe et al., 2004) were multiplied by the optical path length of 6.4 m and mixing ratios of the identified trace gases to reproduce the observed spectrum; the expected spectra were multiplied by -1 (i.e., inverted) prior to presentation. In this example, source 1 emitted ~ 38 ppmv of HONO , ~ 15.5 ppmv of ClNO , ~ 4.0 ppmv of NO_2 and ~ 100 ppmv of H_2O and consumed $> \sim 38$ ppmv of HCl . (B) Expanded view of the 1950 to 1800 cm^{-1} spectral region. The spectrum expected for ~ 4.0 ppmv of NO is superimposed.

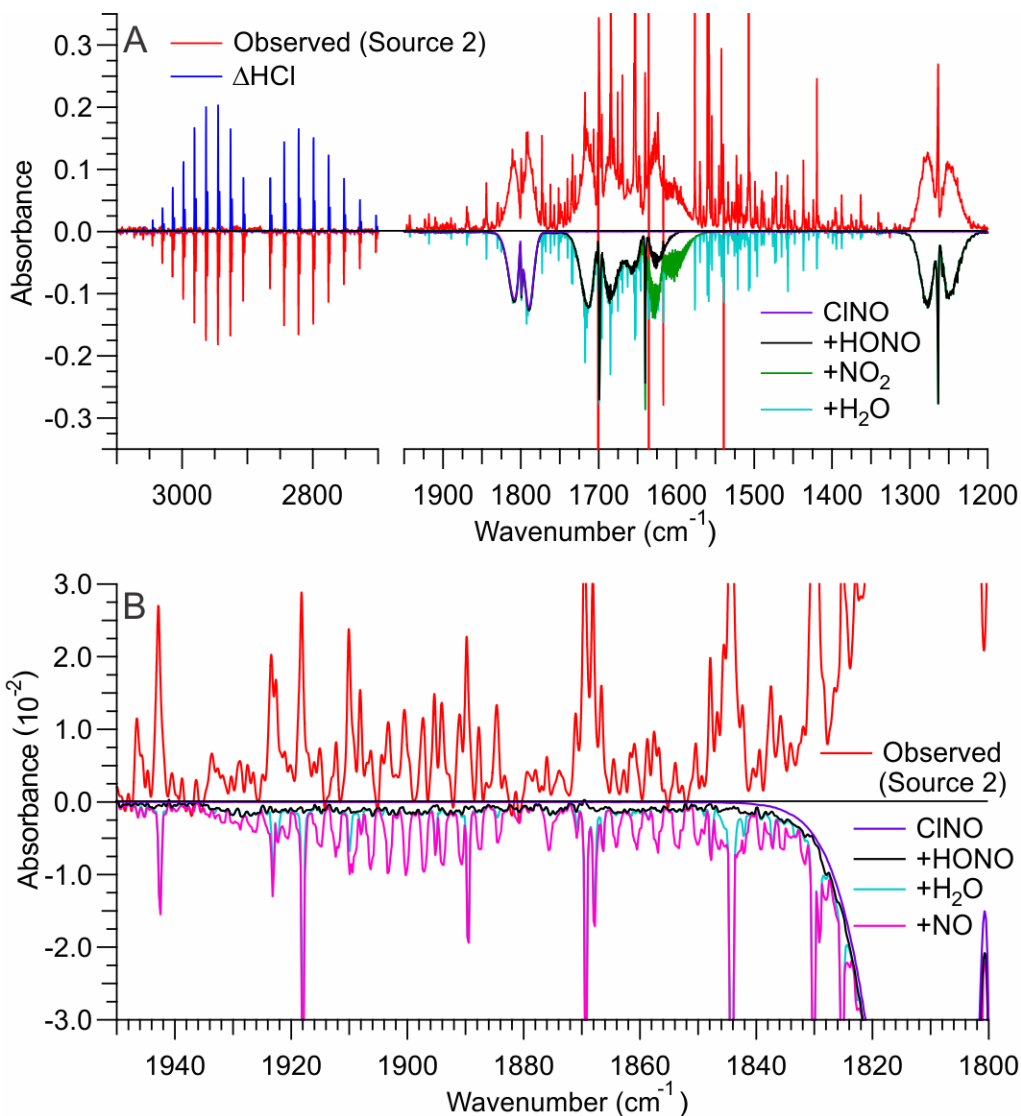


Figure S2. Infrared spectrum (shown in red colour) of a gas stream generated by reaction of HCl_(g) with NaNO_{2(s)} using source 2. In this example, source 2 emitted ~48 ppmv of HONO, ~6.5 ppmv of CINO, ~8.0 ppmv of NO₂ and ~80 ppmv of H₂O and consumed >41.5 ppmv of HCl. (B) An expanded view of the 1950 to 1800 cm⁻¹ spectral region. The spectrum expected for ~8.0 ppmv of NO is superimposed.

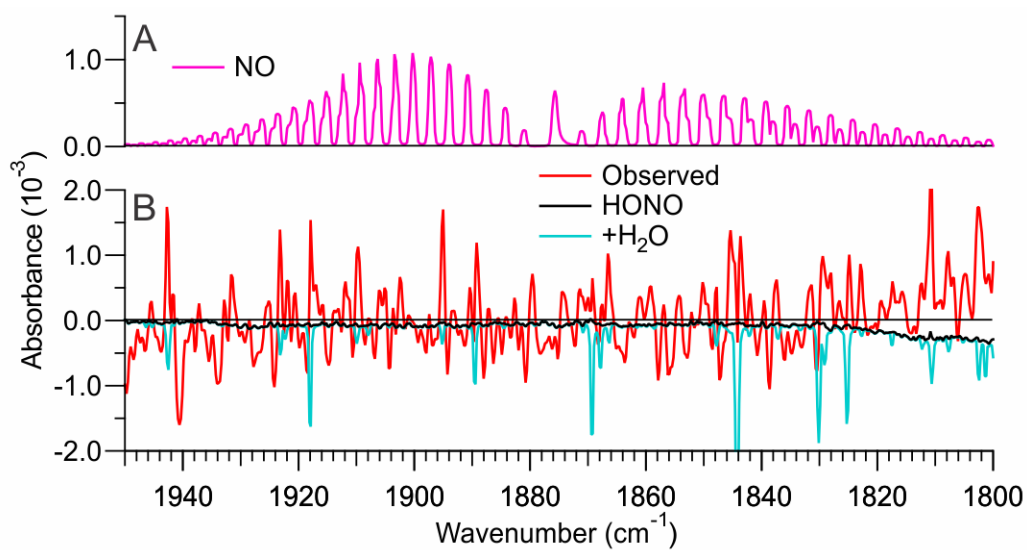


Figure S3. (A) Expected spectrum (Sharpe et al., 2004) for ~1.0 ppmv of NO. (B) Infrared spectrum (shown in red colour) of the optimized source demonstrating the absence of NO.

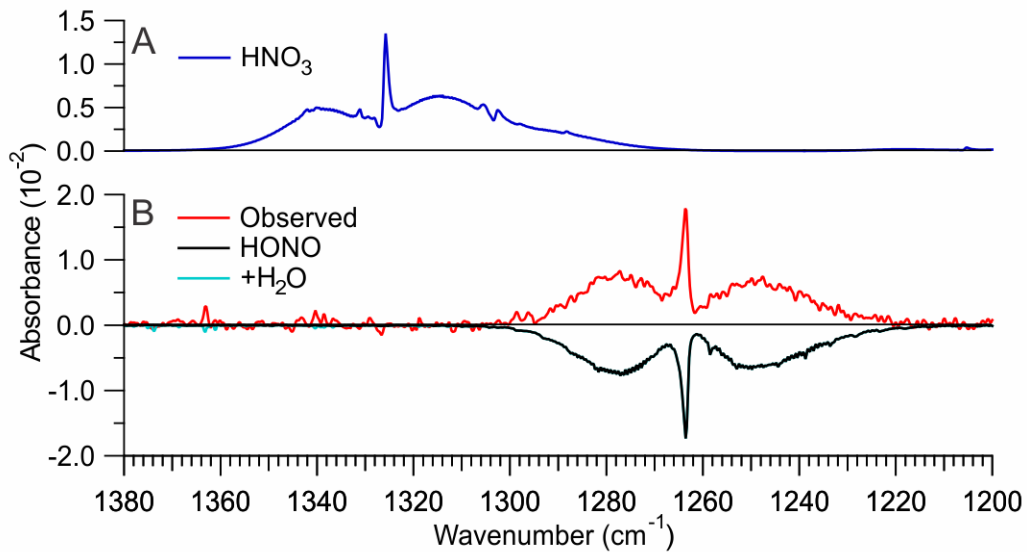
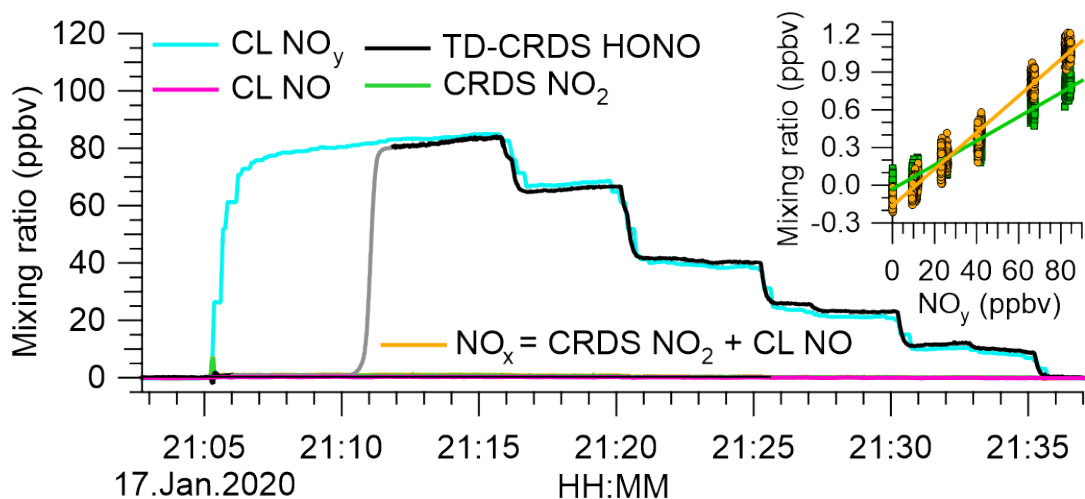


Figure S4. (A) Expected spectrum (Sharpe et al., 2004) for ~1.0 ppmv of HNO₃. (B) Infrared spectrum (shown in red colour) of the optimized source demonstrating the absence of HNO₃.



35

Figure S5. Sample field analysis of the HONO source output. The TD-CRDS and CL instruments sampled scrubbed "zero" air before 21:05 and after 21:36. The HONO source output was added at 21:05:30. Only the CL NO_y responded because the TD-CRDS quartz inlet temperature was 200 °C. At 21:10, the temperature of the quartz inlet was increased from 200 °C to 600 °C to quantify HONO. The absence of an inflection point and prior agreement with the NO_x measurement implies the absence of ClNO. At 21:16 and every ~5 min thereafter, the HONO output concentration was decreased by slightly opening the bypass valve. The insert shows scatter plots of NO₂ and NO_x (calculated by adding CL NO and CRDS NO₂ data) against NO_y. Slopes and offsets were (0.96±0.05)% and -(30±3) pptv for NO₂ (points shown in green) and (1.46±0.08)% and -(164±4) pptv for NO_x (data points shown in orange), respectively.

45

References

Sharpe, S. W., Johnson, T. J., Sams, R. L., Chu, P. M., Rhoderick, G. C., and Johnson, P. A.: Gas-phase databases for quantitative infrared spectroscopy, *Appl. Spectrosc.*, 58, 1452-1461, 2004.